FINAL TECHNICAL REPORT

A FOURIER ANALYSIS OF THE NEAR FIELD VELOCITIES RESULTING FROM A SIMULATED BILATERAL SHEAR FRACTURE

BY

Merle E. Hanson, Allan R. Sanford and Ronald J. Shaffer

January 15, 1971

ARPA Order No.: 1031 Amendment No. 4
Program Code No.: 0F10
Name of Contractor: New Mexico Institute of Mining and Technology
Effective Date of Contract: 18 November 1969
Contract Expiration Date: 17 November 1970
Amount of Contract: $35,000.00
Contract No.: F44620-70-C-0055
Principal Investigator: Merle E. Hanson
Phone: (505) 835-5312
Project Scientist: William J. Best
Phone: (202) 694-5457
Title of Work: Artificial Stimulation of Earthquakes

SPONSORED BY

ADVANCED RESEARCH PROJECTS AGENCY

ARPA ORDER NO. 1031

28

SUMMARY

of the

FINAL TECHNICAL REPORT

on the

CONTRACT

ARTIFICIAL STIMULATION OF EARTHQUAKES

Contract No. F44620-70-C-0055

A FOURIER ANALYSIS OF THE NEAR FIELD VELOCITIES RESULTING FROM A SIMULATED BILATERAL SHEAR FRACTURE

The purpose of this project is to analyze the dynamic stress fields in geologic media particularly those created by fracture or other dynamic source functions. Lack of realistic analytic descriptions has led to the study of dynamic fracture in strained elastic media. An added goal is to aid the observational seismologist in the interpretation of transient data from real seismic events for the description of source type and source parameters.

A two dimensional simulation of a dynamic shear fracture was performed and reported earlier in the contract year. The velocities at several points in the near field have been Fourier analyzed to determine the amplitude characteristics resulting from the bilateral shear fracture.

The holes in the amplitude spectrums of the velocity data in the near field are compared with an analytically calculated source time. The periods resulting from the holes in the amplitude spectrums correlate with the source time calculated from analytical considerations. There is, however, the added complications of the near field which results in both of the body wave speeds affecting some of the points. The radiation from either side of the bilateral fracture can affect the points being observed. The calculated time trace was not of sufficient length to indicate whether the complete spectrum was determined. The study indicates that the spectrum analysis of the near field velocities can show at least part of the characteristics of the finite source.

A FOURIER ANALYSIS OF THE NEAR FIELD VELOCITIES
RESULTING FROM A SIMULATED BILATERAL SHEAR FRACTURE

By
Merle E. Hanson, Allan R. Sanford, Ronald J. Shaffer

ABSTRACT

The data from a numerically simulated dynamic bilateral shear fracture was analyzed using Fourier spectral techniques. The holes in the amplitude spectrums of the velocity data in the near field are compared with an analytically calculated source time. The periods resulting from the holes in the amplitude spectrum correlate with the source time calculated from analytical considerations. The analysis of the near field velocities at an observation point can show at least part of the characteristics of the finite source.

INTRODUCTION

Several authors, e.g., Davies and Smith (1968), have shown that amplitude properties of body waves can be used to determine source parameters such as fault area and fracture velocity. Most of these studies have been applied to data retrieved at distances from the source that are large compared to the dimensions of the source. In addition, they have been primarily concerned with frequencies lying within a narrow band width.

In our research, amplitude and phase spectra have been obtained for the near field velocities associated with a simulated bilateral shear fracture. A discussion of some of the characteristics of the dynamic shear fracture are given by Hanson, Sanford, and Shaffer (1971). The apparent duration of fracture at a point away from the fracture (hereafter called source time) had to be defined for radial distances from the fracture comparable to the fracture length. Two-space dimensions were considered with the particle velocities determined perpendicular ($\dot{v}$) and parallel ($\dot{u}$) to the plane of the fracture.

TECHNIQUE

The simulated fracture described by Hanson, Sanford, and Shaffer (1971) formed in a block of brittle elastic material infinite in the z direction (plane strain). The block was initially subjected to shearing and normal stresses.

A fracture nucleus formed at the center of the block ($x = 0$, $y = 0$) at $t = 0$ and propagated bilaterally along the x-axis. The normal stresses were adjusted so that the fracture axis was an axis of maximum shear stress. The fracture was made to travel at constant velocity, 0.4 of the P-wave velocity, for a given length and stop. The final half-crack length chosen was 7 centimeters. The Lamé constants and the density chosen resulted in a P-wave velocity of 0.33333 cm/microsecond and an S-wave speed of 0.19245 cm/microsecond. Fracture acceleration and deceleration were not included in the model study. The calculation was terminated before reflections from mesh boundaries would affect the velocity histories of the points which were spectrum analyzed.

A two-dimensional dynamic velocity data was generated in the two-directions, parallel ($\dot{u}$) and perpendicular ($\dot{v}$) to the fracture, for all the mesh points in the grid by the model. This data was stored in digital form with uniform time spacing. Examination of the figures 2-11 shows that the velocity time series were 213.75 microseconds long with 171 discrete data samples per trace. A digital form of the Fourier transform

$$A(k) = \sum_{n=0}^{N} a_n \cos\left(\frac{\pi k n}{m}\right) \Delta t - i\sum_{n=0}^{N} a_n \sin\left(\frac{\pi k n}{m}\right) \Delta t \qquad (1)$$

$$k = 0, 1, 2, \ldots\ldots, m$$

was used, where N represents the total number of data samples per trace and m was chosen so that the maximum frequency on the figures is about 1/2 the Nyquist frequency. The frequency is 0.00117 k cycles/microsecond where k is defined above.

Theoretical studies (Ben-Menahem, 1962) indicate that the velocity spectrum should include a factor of the form (sin sin $\pi fT)/\pi fT$ approximately. This factor is an indication of the finiteness of the size of the source and will produce holes in the amplitude spectrum when $fT = n$, or for the first harmonic when the period $\tau = T$. For the near field the form taken here for an indicated source time T is taken as

$$T^{(R)} = T_f + \frac{R_o}{C^{(2)}} \sqrt{1 - \frac{2b}{R_o} \cos \Theta + \left(\frac{b}{R_o}\right)^2} - \frac{R_o}{C^{(1)}} ,$$

and (2)

$$T^{(L)} = T_f + \frac{R_o}{C^{(2)}} \sqrt{1 + \frac{2b}{R_o} \cos \Theta + \left(\frac{b}{R_o}\right)^2} - \frac{R_o}{C^{(1)}} ,$$

where $T^{(R)}$ is the source time (as measured from the right hand tip of the bilateral fracture) for the right half of the fracture and $T^{(L)}$ is the source time for the left half of the fracture. T_f is the actual source time from start of fracture propagation to completion of fracture, R_o is the radial distance from the center of the fracture to the point, Θ is the angle measured from the fracture axis to the radius R_o, and b is the half crack length. $C^{(1)}$ and $C^{(2)}$ are body wave speeds with the superscripts 1 and 2 indicating a path from the center and ends of the crack, respectively.

Normally, separate amplitude spectra are obtained for P and S waves. This means that only a single velocity need be considered in the interpretation of the spectra. In this report, the spectra include both P and S waves. Therefore, the interpretation of the holes becomes very much more complicated because of the interaction of P and S waves. For our spectra, there are four rather than two possible source times to consider for each spectra.

The points analyzed by spectral techniques were chosen to be only in the upper right hand quadrant. The point of fracture nucleation is the origin of the coordinate system and the fracture lies along the x axis.

DISCUSSION OF RESULTS

Shown in this paper are the two velocities and their amplitude spectrums for 5 points spaced about the crack in the upper right hand quadrant. The observation points were chosen so that the angle Θ measured from the positive x axis varied from 19 to 90 degrees. Figure 1 shows the fracture and the observation points approximately to scale for the two dimensional simulation.

Figures 2-11 show the velocity in the u and v directions as a function of time and the associated amplitude spectrum plots for the five observation points near the bilateral shear crack. Table 1 gives the angle between the x-axis and the line from the center of the fracture to the point, the

associated radius from the fracture center and the source time from equation 2 best fitting the first observed hole in the spectra. The last column in Table 1 indicates whether the hole arises from movement on the left side or the right side of the fracture.

Figures 2 and 3 show the velocity and amplitudes for R_o = 12.5 cm and Θ = 90°. All the amplitude spectra indicate significant movement at the lower frequencies. This may be partly due to the truncation of the time series used. However, the time traces of the particle velocities indicate plenty of low frequency motion. The parallel velocity trace shows a significant hole at K = 15 corresponding to a period of 57 microseconds (see Table 1). Equation 2 (using the shear wave speed for $C^{(1)}$ and the compressional wave speed for $C^{(2)}$) results in a time T of 58 microseconds. The direction of the shear field is toward the right above the fracture. It is possible that there could also be a hole at lower frequency resulting from the exclusive use of shear wave speeds in the equation. In this case, however, the time series was not of sufficient length to show this hole. $\dot{v}$ at this point does not exhibit any strong holes in its amplitude spectrum. There is a weak hole at K = 30 corresponding to a period of 29 microseconds. This corresponds to shear wave body speed from the fracture center and compressional body wave speed from both of the stopped tips.

An example of where a hole is not well defined is the spectra of $\dot{u}$ at the point 3 (R_o = 14.3 and Θ = 61°) Figures 6 and 7. From Table 1, it can be observed that the correlation of the hole at K = 35.3, a period of 24 microseconds, is not good with the closest value of T calculated from Equation 2. In addition the hole in the spectrum is weak. For this point, $\dot{v}$ exhibits a fairly well defined hole in its amplitude spectrum at K = 14, at a period of 61 microseconds. This corresponds to the time T (65 microseconds) obtained from Equation 2 when the compressional body wave speeds are used for both $C^{(1)}$ and $C^{(2)}$. The hole in the spectrum in this case results from the radiation from the left half of the fracture.

The point 2 (R_o = 22.7 and Θ = 33°) shows two holes in the spectrum of $\dot{u}$ at K = 12 and 25.2, which corresponds to periods of 71 and 34 microseconds, respectively (see Figures 8 and 9). Using Equation 2, it can be seen from Table 1 that the first hole results from radiation from the left side of the fracture and the second hole results from radiation from the right side of the fracture. In both cases, the compressional wave speed was used for $C^{(1)}$ and $C^{(2)}$. $\dot{v}$ exhibits a similar pattern for similar reasons. On the other hand, it can be seen fro Table 1 that the first hole is the result of shear wave radiation from the left half of the fracture.

Similar discussions can be made for the other points. Results are given in Table 1. In general, $\dot{u}$ directly above the right tip does not exhibit any well defined holes. This probably occurs because of the complicated overlapping of the radiation patterns.

Complete interpretations of the spectrum have not been made, primarily because a longer time series should be used to determine the amplitude spectrums. This procedure was not possible in this case as a larger computer is required to simulate the dynamic phenomena. However, the amplitude spectrum of the near field velocities presented here will show at least part of the character of the finite source.

CONCLUSIONS

The analysis of the amplitude spectrum shows that the spectrum of the near field velocities at an observation point can show at least part of the characteristics of the finite source. The time series generated by the simulated two-dimensional dynamic shear fracture was not of sufficient length to show conclusively that there are not holes in the spectrum at longer periods. As can be seen from the graphs of particle velocity, the duration of the time series is approximately the same length as the fundamental wavelength. A longer time series would reduce some of the erroneous amplitude information arising from truncation of the time series.

Application of the spectrum techniques to near field data with known simulated fracture phenomena may provide a method of determining source parameters for real seismic events. However, longer time series (a greater number of discrete data points) are required. This imposes a restriction that the simulation will require a larger grid, hence larger computers and longer computer times.

ACKNOWLEDGEMENTS

The authors wish to express their appreciation to Mr. Thomas Schellhase who assisted in developing the computer plot and Fourier spectrum analysis routines. This research was supported by the Advanced Research Projects Agency of the Department of Defense and was monitored by the Air Force Office of Scientific Research under Contract Number F44620-70-C-0055.

BIBLIOGRAPHY

Ben-Menahem, A. 1962. Radiation of seismic body waves from a finite moving source in the earth, Jour. Geophys. Res., 67, 345-350.

Davies, J. B. and Smith, S. W. 1968. Source parameters of earthquakes and discrimination between earthquakes and nuclear explosions, Bull. Seis. Soc. Am., 58, 1503-1517.

Hanson, M. E., Sanford, A. R. and Shaffer, R. J. 1971. A source function for a dynamic bilateral brittle shear fracture, in press.

T A B L E 1

	VELOCITY COMPONENT	r_o cm	Θ DEGREES	SHEAR OR COMPRESSIONAL WAVE		T (microsecond) FROM		TIP FROM WHICH HOLE WAS GENERATED
				$C^{(1)}$	$C^{(2)}$	EQUATION 2	FOURIER SPECTRUM	
1*	Parallel	13.8	19	shear	comp.	42.5	42.8	left
	Perpendicular	13.8	19	shear	shear	87.5	85.5	left
		13.8	19	shear	comp.	42.5	43.5	left
2*	Parallel	22.7	33	comp.	comp.	71	71	left
		22.7	33	comp.	comp.	36.3	34	right
	Perpendicular	22.7	33	shear	shear	84.2	85	left
		22.7	33	comp.	comp.	36.3	37	right
3*	Parallel	14.3	61	shear	comp.	15.6	24	right
	Perpendicular	14.3	61	comp.	comp.	65.8	61	left
4*	Parallel	13.1	72.5	shear	shear	51	50	right
	Perpendicular	13.1	72.5	shear	shear	71	68	left
		13.1	72.5	shear	comp.	34	36	left
5*	Parallel	12.5	90	comp.	comp.	58	57	left or right
	Perpendicular	12.5	90	shear	comp.	31	29	left or right

*Reference points in Figure 1.

FIGURE CAPTIONS

FIGURE 1--Sketch approximately to scale of the geometry of the fracture and the observation points whose velocities were Fourier analyzed. The initial shear field and the angle Θ used in Equation 2 are displayed.

FIGURE 2--The parallel velocity ($\dot{u}$) and the associated amplitude spectrum for point 5 on Figure 1, the time on the velocity plot is in microseconds.

FIGURE 3--The perpendicular velocity ($\dot{v}$) and the associated amplitude spectrum for point 5 on Figure 1, Θ the time on the velocity plot is in microseconds.

FIGURE 4--The parallel velocity ($\dot{u}$) and the associated amplitude spectrum for point 4 on Figure 1, the time on the velocity plot is in microseconds.

FIGURE 5--The perpendicular velocity ($\dot{v}$) and the associated amplitude spectrum for point 4 on Figure 1, the time on the velocity plot is in microseconds.

FIGURE 6--The parallel velocity ($\dot{u}$) and the associated amplitude spectrum for point 3 on Figure 1, the time on the velocity plot is in microseconds.

FIGURE 7--The perpendicular velocity ($\dot{v}$) and the associated amplitude spectrum for point 3 on Figure 1, the time on the velocity plot is in microseconds.

FIGURE 8--The parallel velocity ($\dot{u}$) and the associated amplitude spectrum for point 2 on Figure 1, the time on the velocity plot is in microseconds.

FIGURE 9--The perpendicular velocity ($\dot{v}$) and the associated amplitude spectrum for point 2 on Figure 1, the time on the velocity plot is in microseconds.

FIGURE 10--The parallel velocity ($\dot{u}$) and the associated amplitude spectrum for point 1 on Figure 1, the time on the velocity plot is in microseconds. The high frequency oscillation seen on the velocity is the calculational grid noise from the numerical model.

FIGURE 11--The perpendicular velocity ($\dot{v}$) and the associated amplitude spectrum for point 1 on Figure 1, the time on the velocity plot is in microseconds.

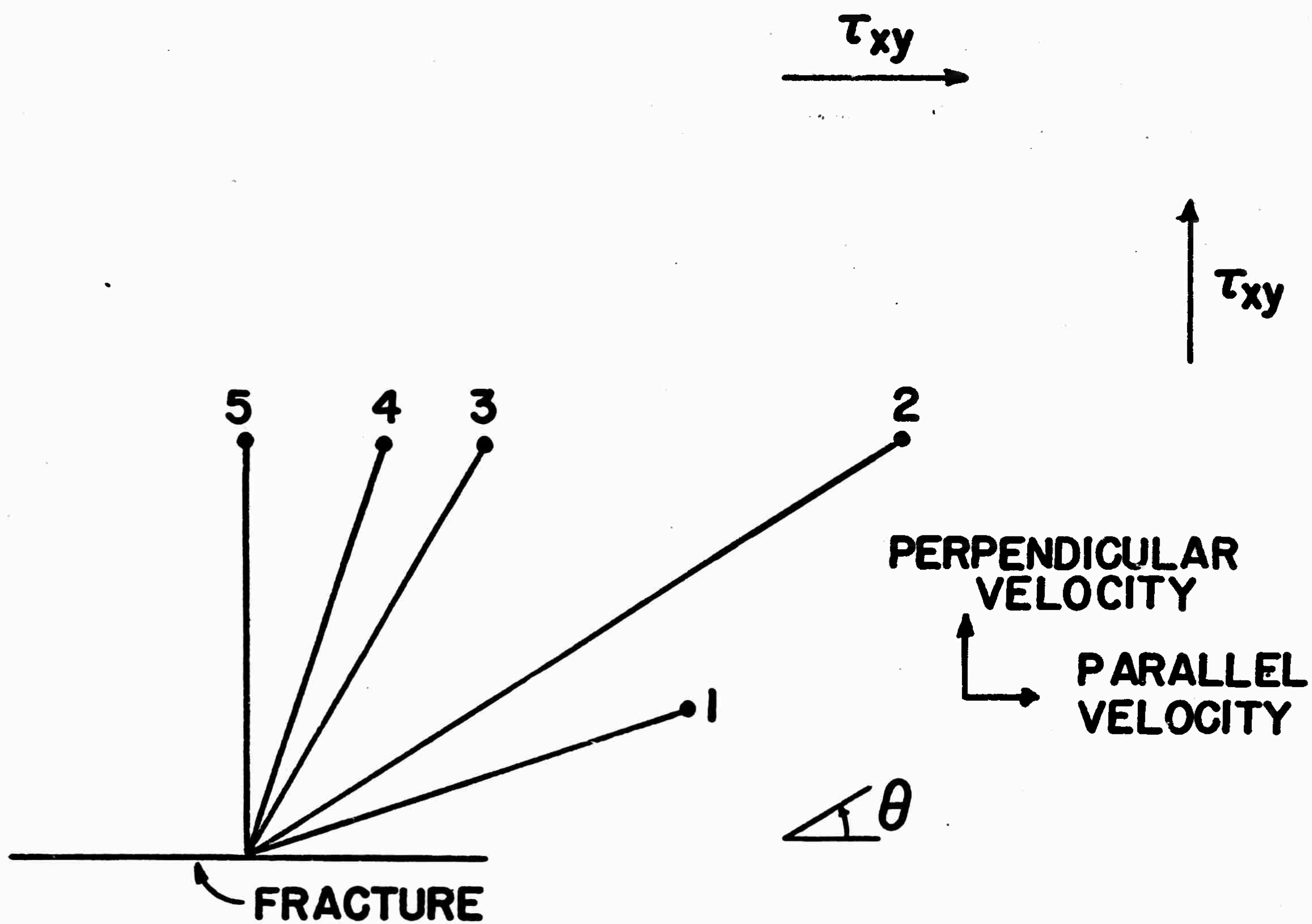

τxy
τxy
5
4
3
2
1
PERPENDICULAR VELOCITY
PARALLEL VELOCITY
θ
FRACTURE

FIG 1

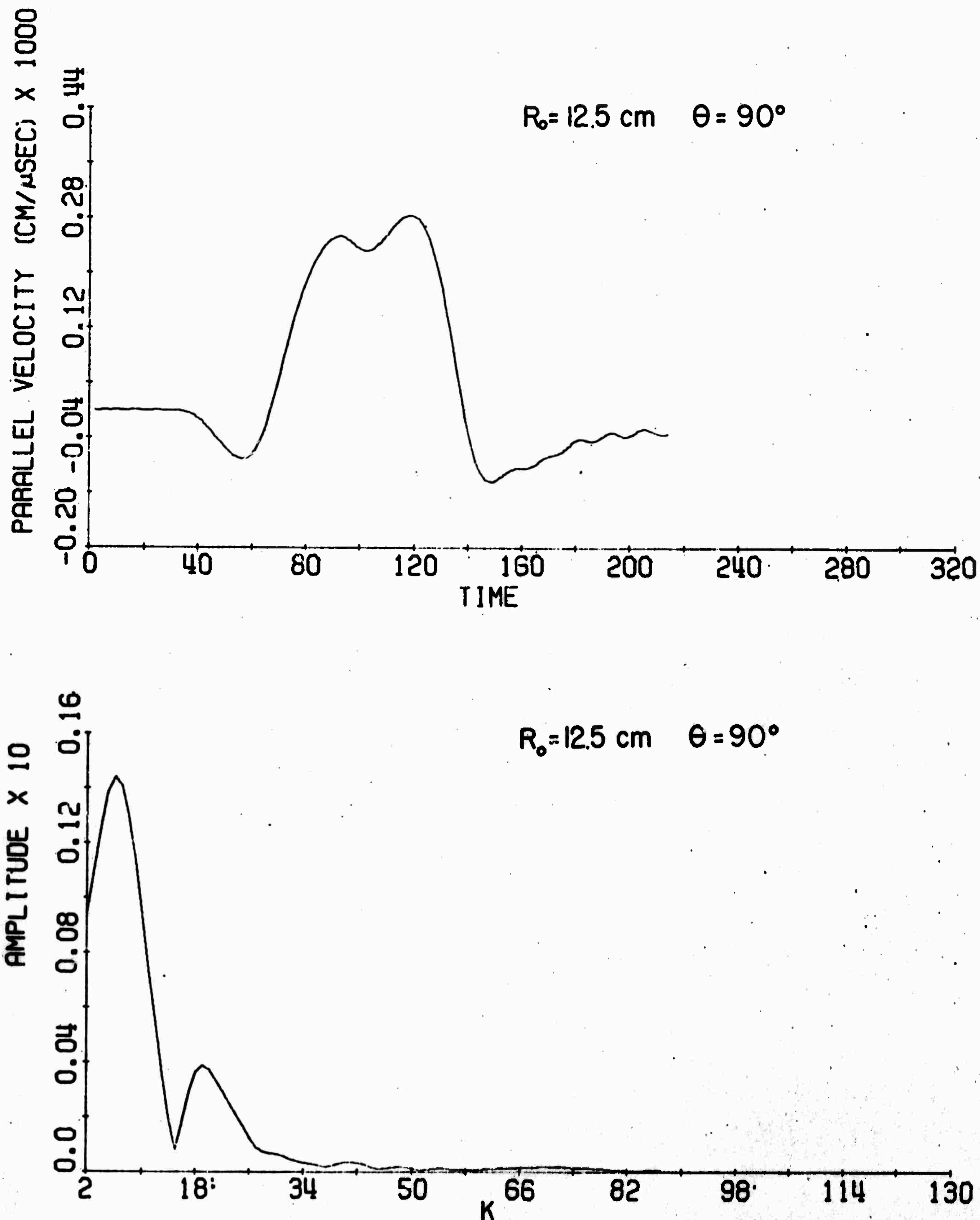
PARALLEL VELOCITY (CM/µSEC) X 1000
R_o= 12.5 cm θ = 90°
-0.20
-0.04
0.12
0.28
0.44
0
40
80
120
160
200
240
280
320
TIME
AMPLITUDE X 10
R_o= 12.5 cm θ = 90°
0.0
0.04
0.08
0.12
0.16
2
18
34
50
66
82
98
114
130
K

FIG. 2

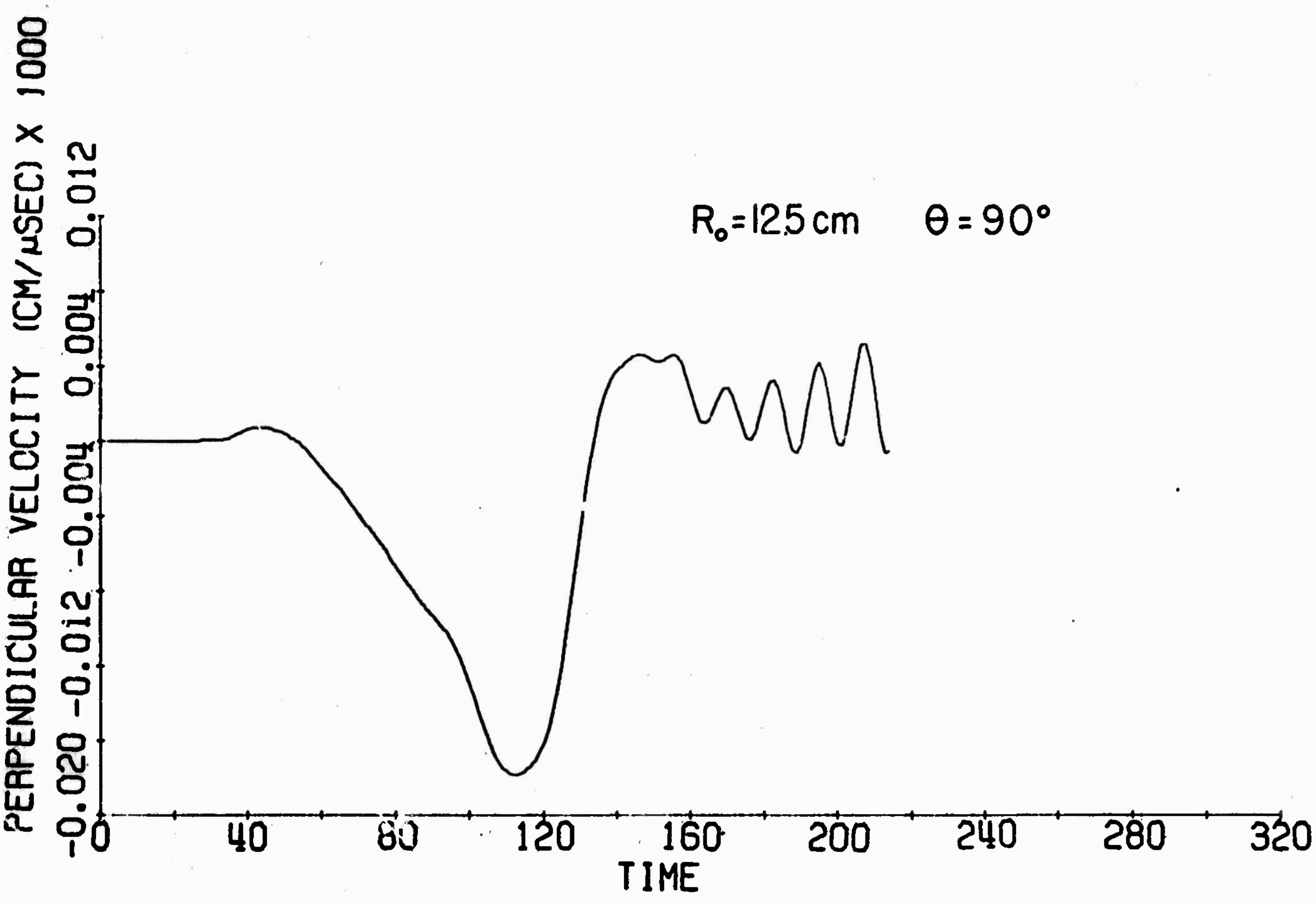

PERPENDICULAR VELOCITY (CM/μSEC) X 1000
-0.020 -0.012 -0.004 0.004 0.012
R_o=12.5 cm θ=90°
0 40 80 120 160 200 240 280 320
TIME

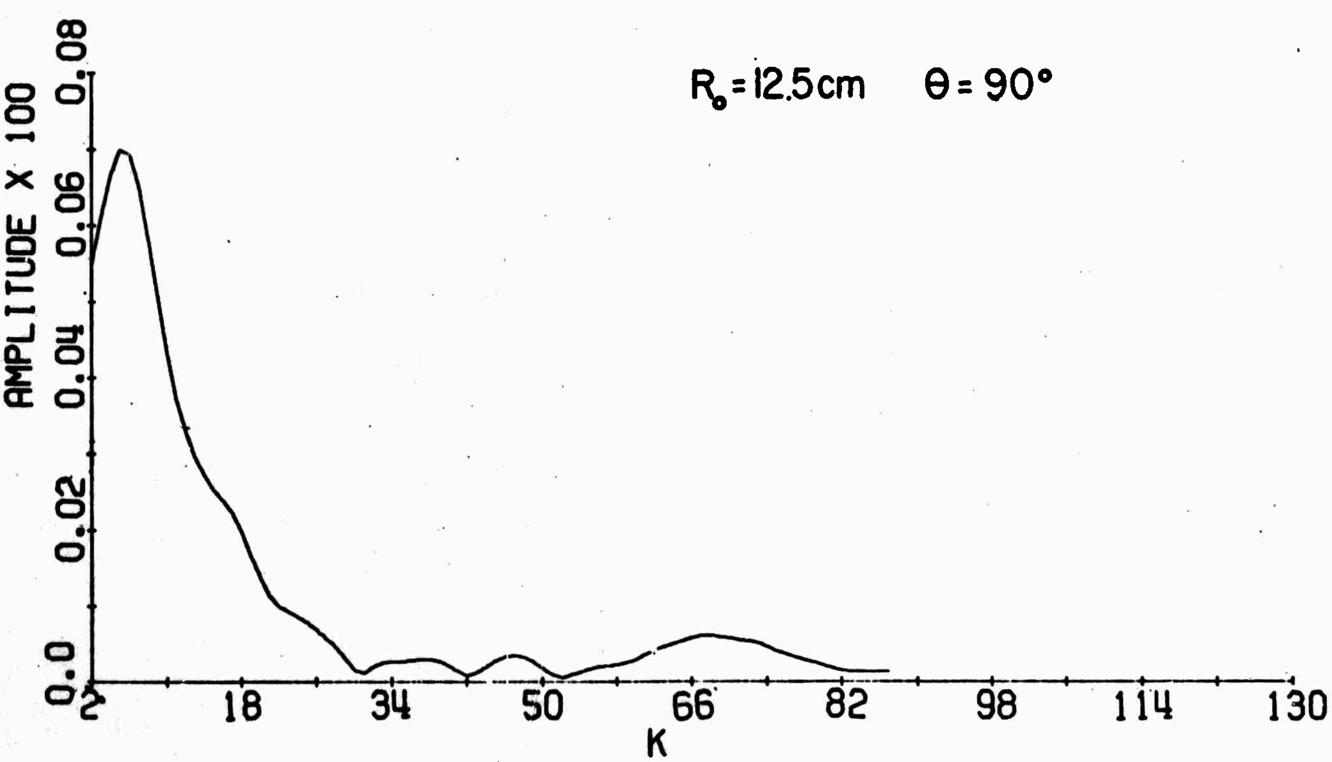

AMPLITUDE X 100
0.0 0.02 0.04 0.06 0.08
R_o=12.5cm θ=90°
2 18 34 50 66 82 98 114 130
K

FIG 3

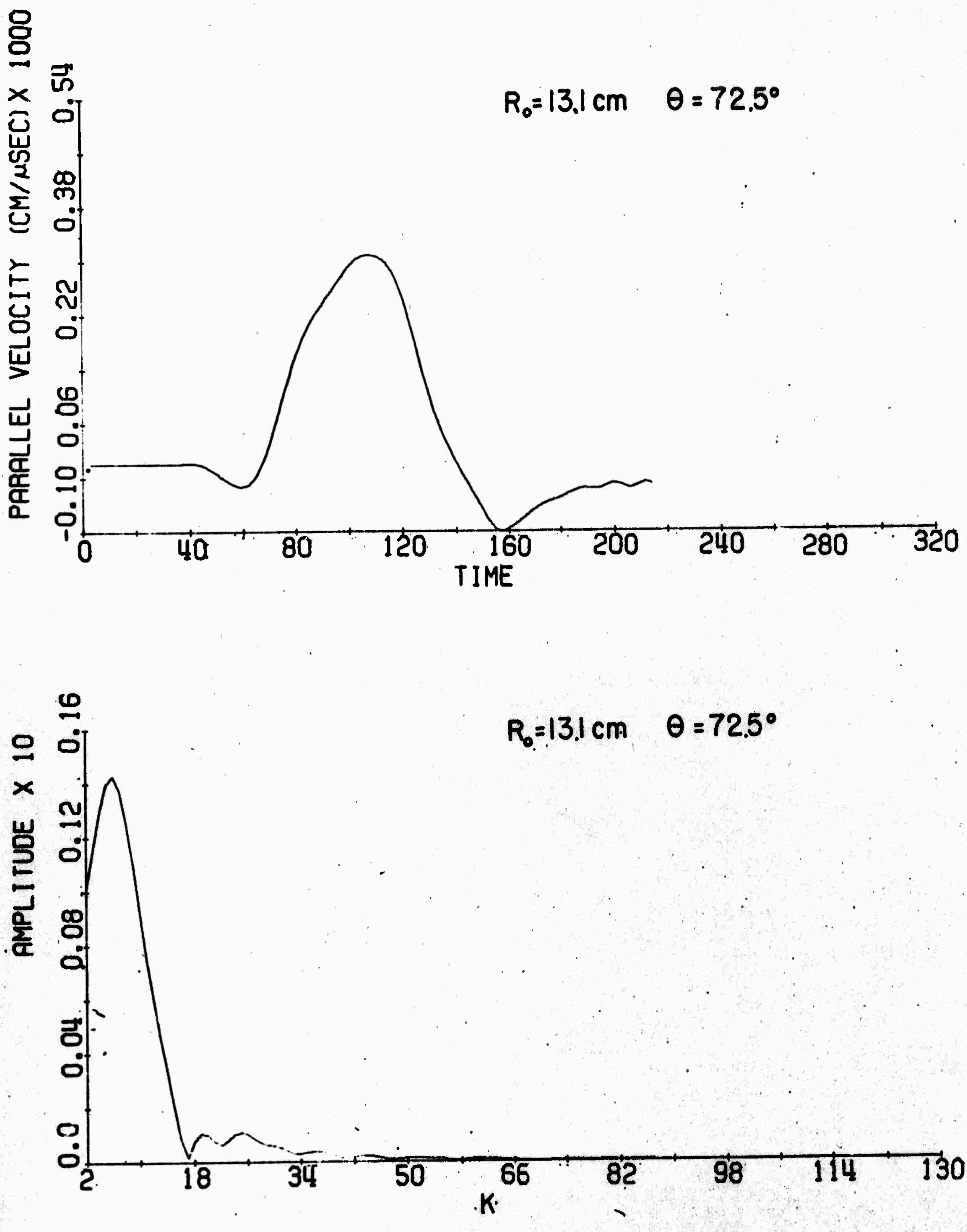

PARALLEL VELOCITY (CM/μSEC) X 1000
-0.10 0.06 0.22 0.38 0.54
R_o=13.1 cm   θ = 72.5°
0 40 80 120 160 200 240 280 320
TIME
AMPLITUDE X 10
0.0 0.04 0.08 0.12 0.16
R_o=13.1 cm   θ = 72.5°
2 18 34 50 66 82 98 114 130
K

FIG. 4

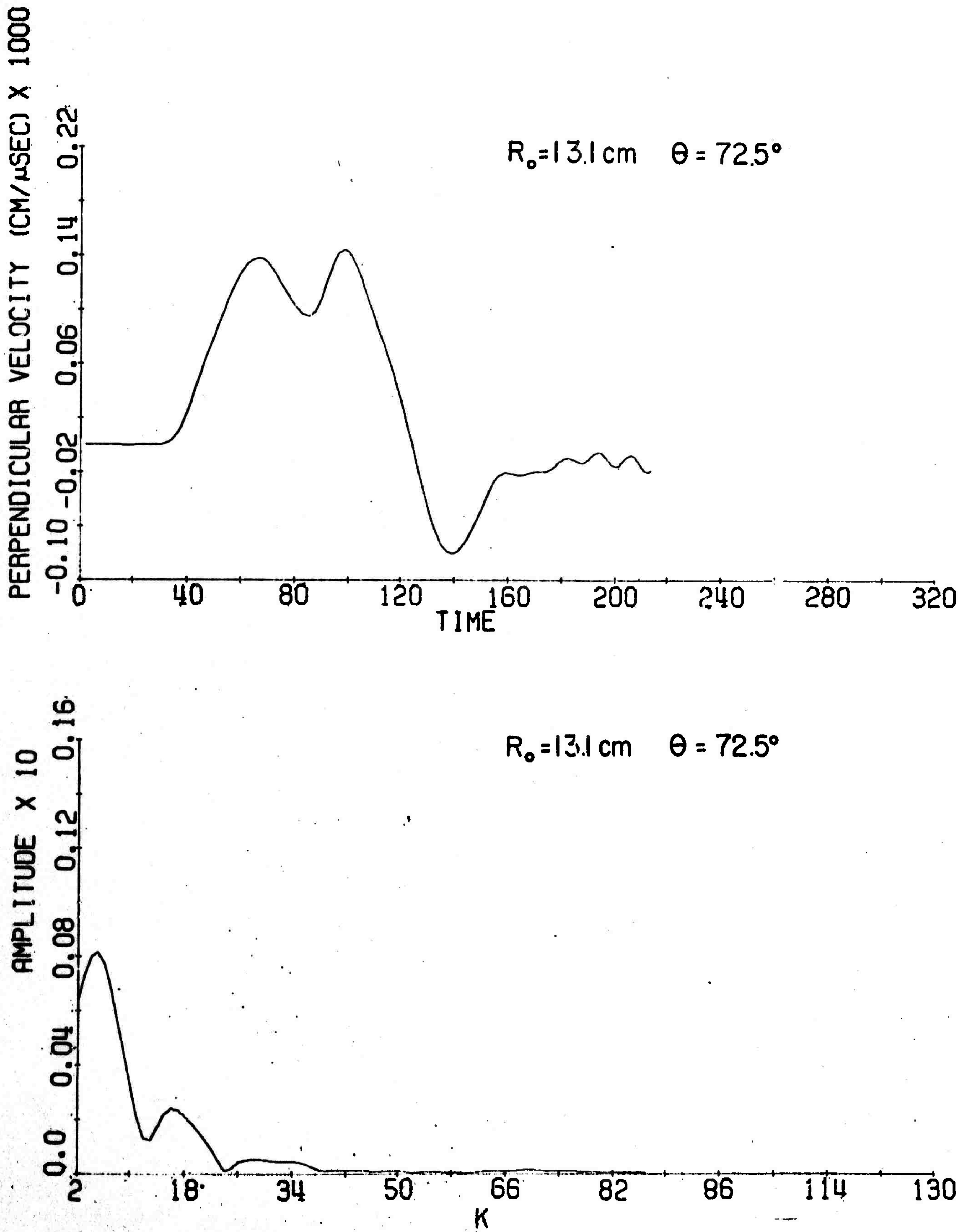
PERPENDICULAR VELOCITY (CM/μSEC) X 1000
-0.10 -0.02 0.06 0.14 0.22
R_o=13.1 cm θ = 72.5°
0 40 80 120 160 200 240 280 320
TIME
AMPLITUDE X 10
0.0 0.04 0.08 0.12 0.16
R_o=13.1 cm θ = 72.5°
2 18 34 50 66 82 86 114 130
K

FIG. 5

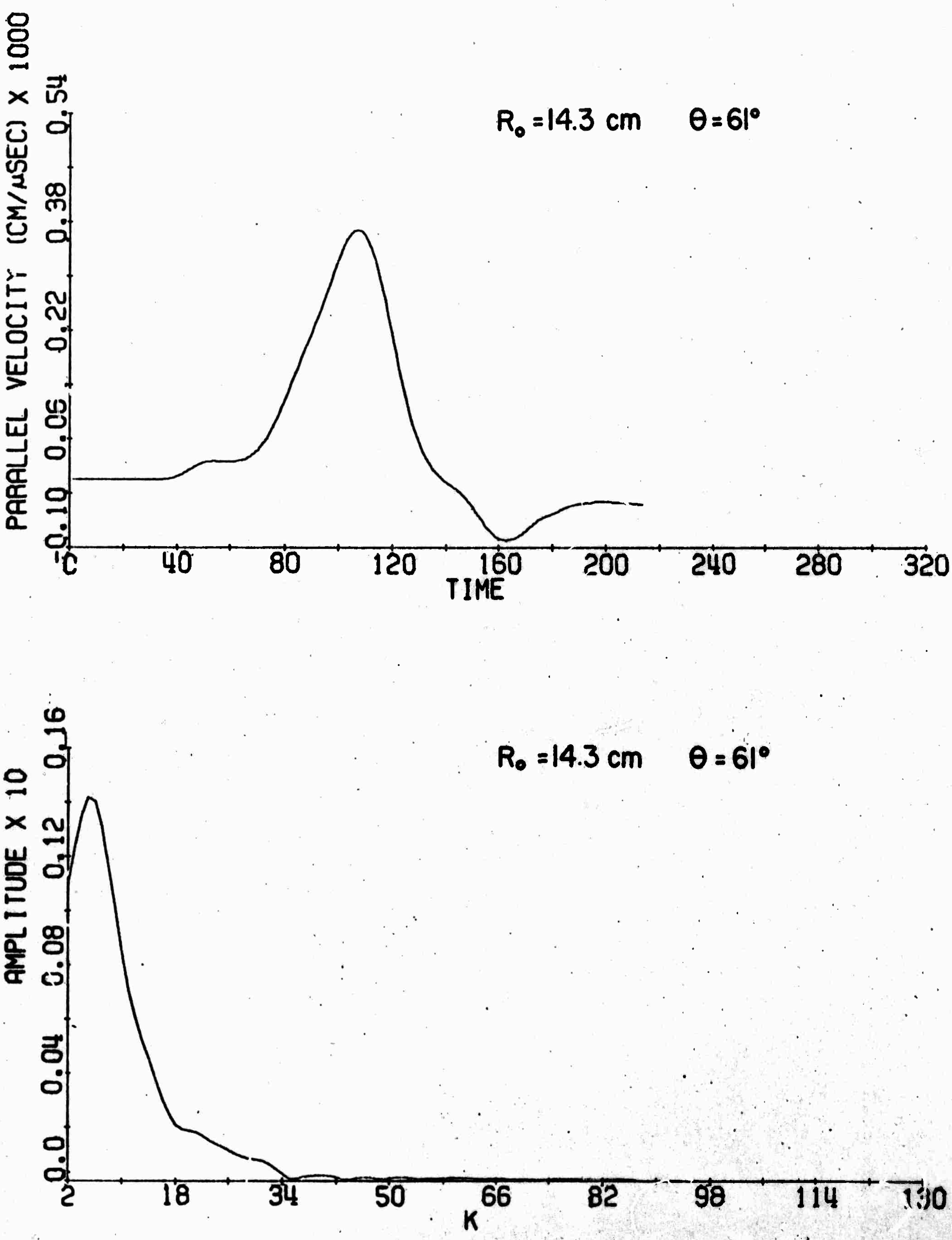

PARALLEL VELOCITY (CM/μSEC) X 1000
R_o =14.3 cm θ=61°
-0.10 -0.10 0.06 0.22 0.38 0.54
0 40 80 120 160 200 240 280 320
TIME
AMPLITUDE X 10
R_o =14.3 cm θ=61°
0.0 0.04 0.08 0.12 0.16
2 18 34 50 66 82 98 114 130
K

FIG. 6

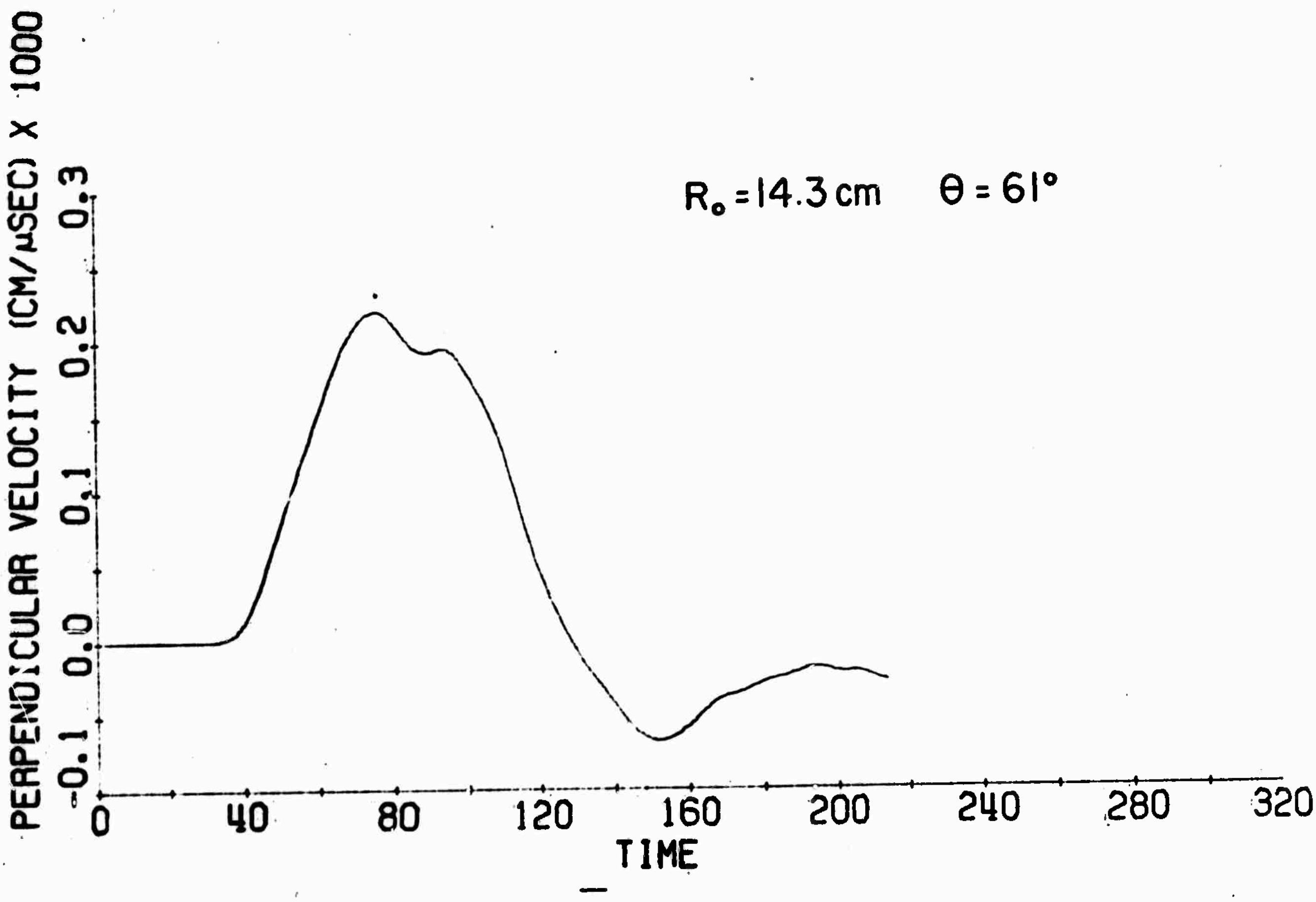
PERPENDICULAR VELOCITY (CM/μSEC) X 1000
R_o = 14.3 cm θ = 61°
-0.1
0.0
0.1
0.2
0.3
0
40
80
120
160
200
240
280
320
TIME

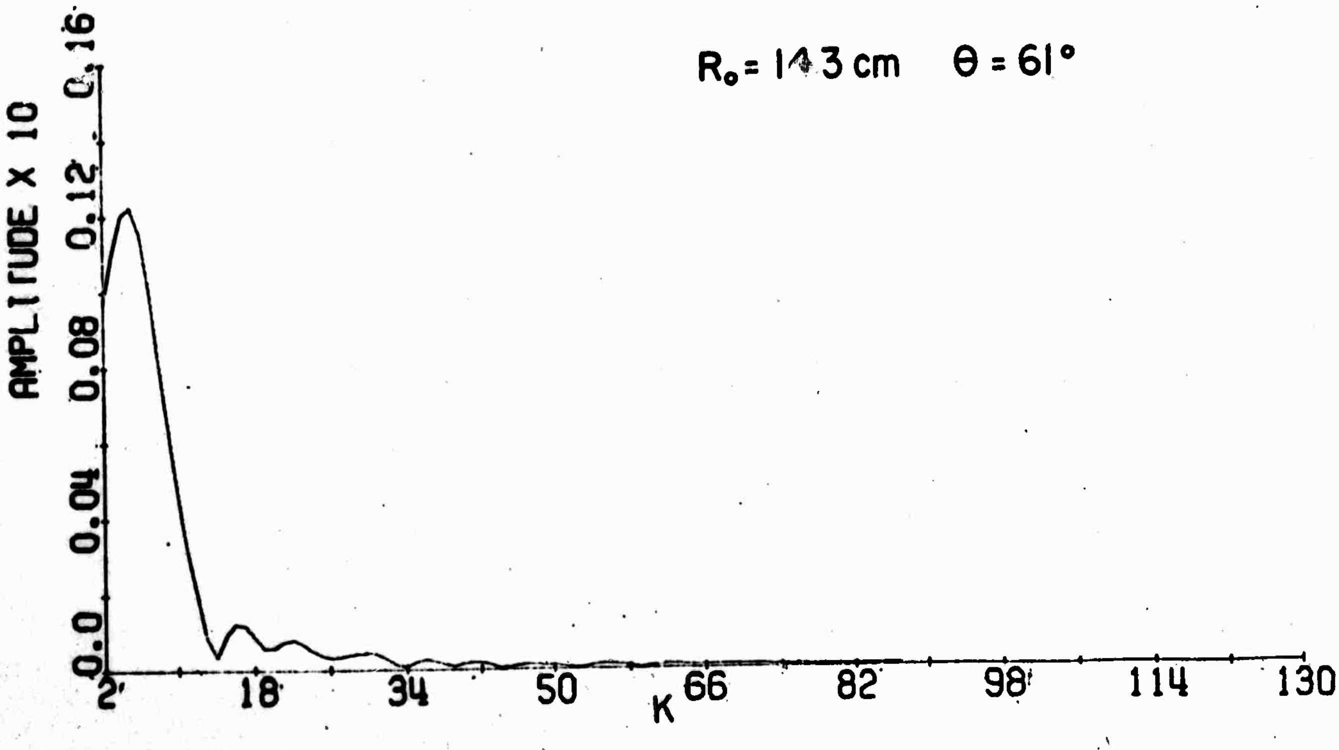
AMPLITUDE X 10
R_o = 14.3 cm θ = 61°
0.0
0.04
0.08
0.12
0.16
2
18
34
50
66
82
98
114
130
K

FIG. 7

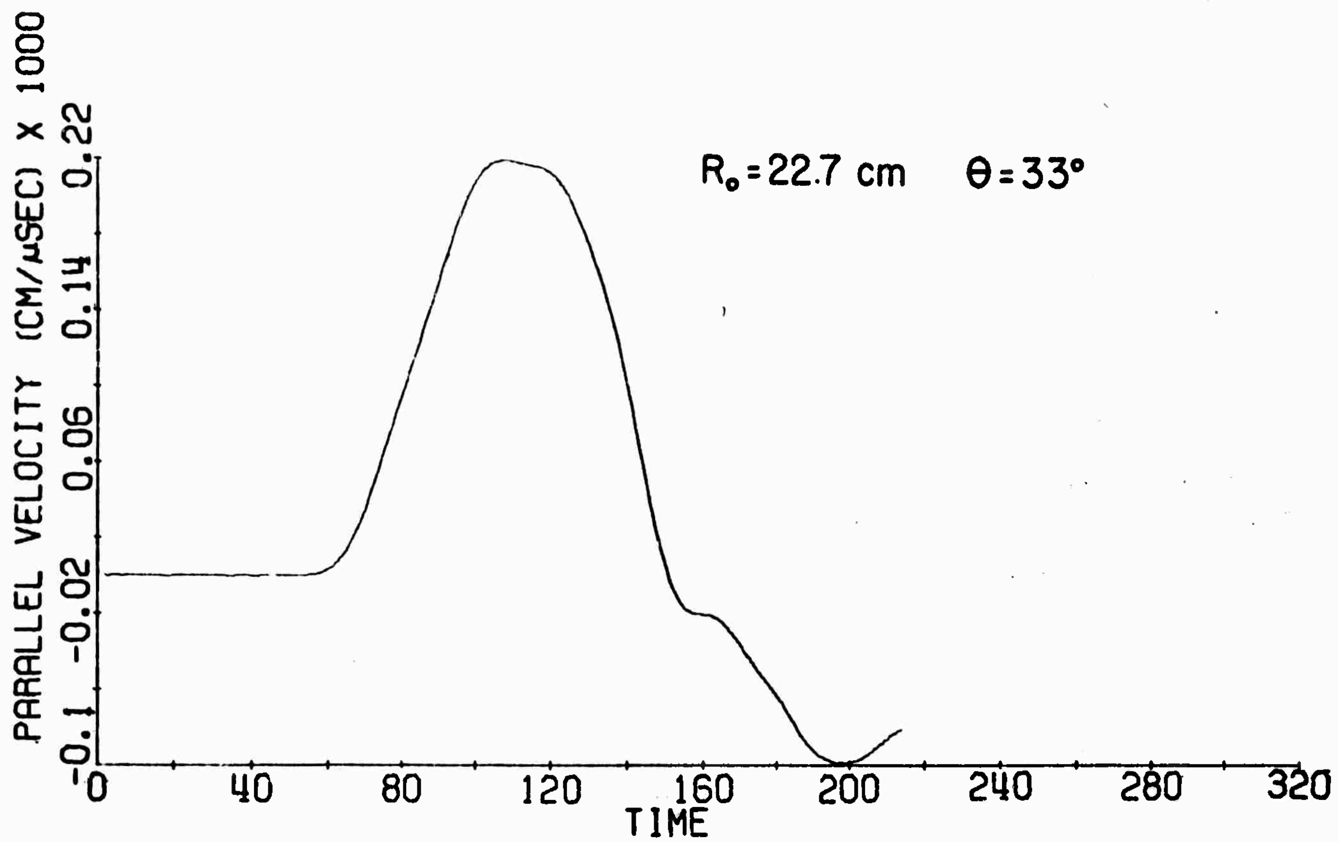

PARALLEL VELOCITY (CM/µSEC) X 1000
R_o=22.7 cm θ=33°
-0.1
-0.02
0.06
0.14
0.22
0
40
80
120
160
200
240
280
320
TIME

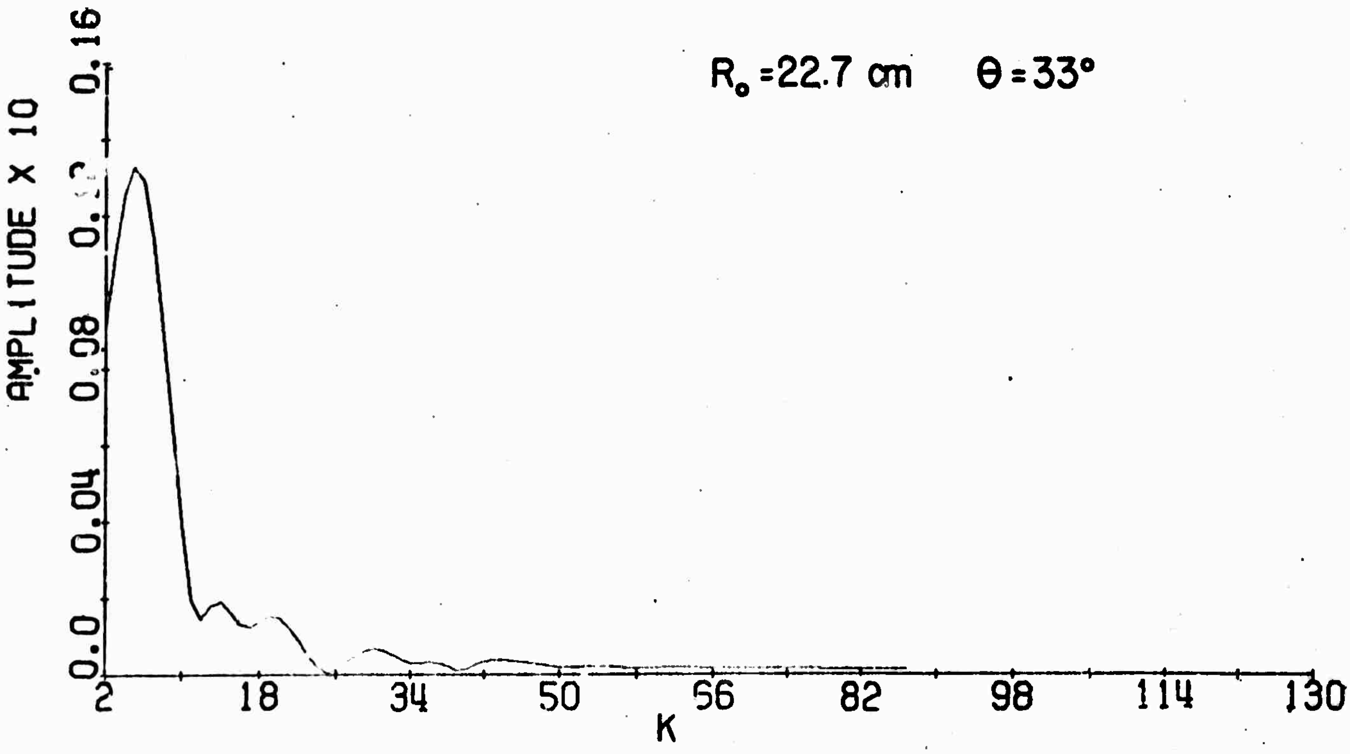

AMPLITUDE X 10
R_o=22.7 cm θ=33°
0.0
0.04
0.08
0.16
2
18
34
50
66
82
98
114
130
K

FIG. 8

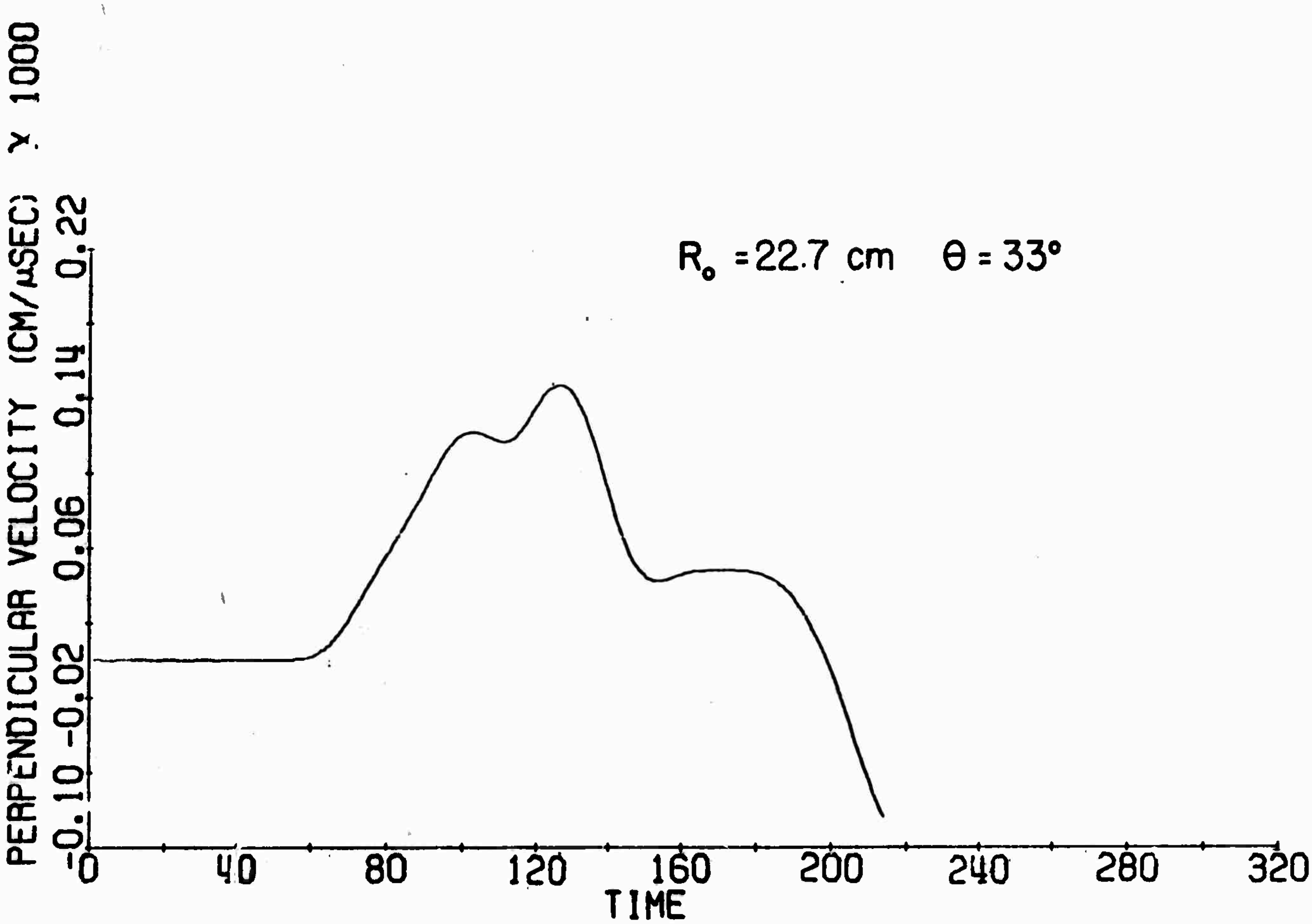

PERPENDICULAR VELOCITY (CM/μSEC) X 1000
-0.18 -0.10 -0.02 0.06 0.14 0.22
R₀ =22.7 cm θ = 33°
0 40 80 120 160 200 240 280 320
TIME

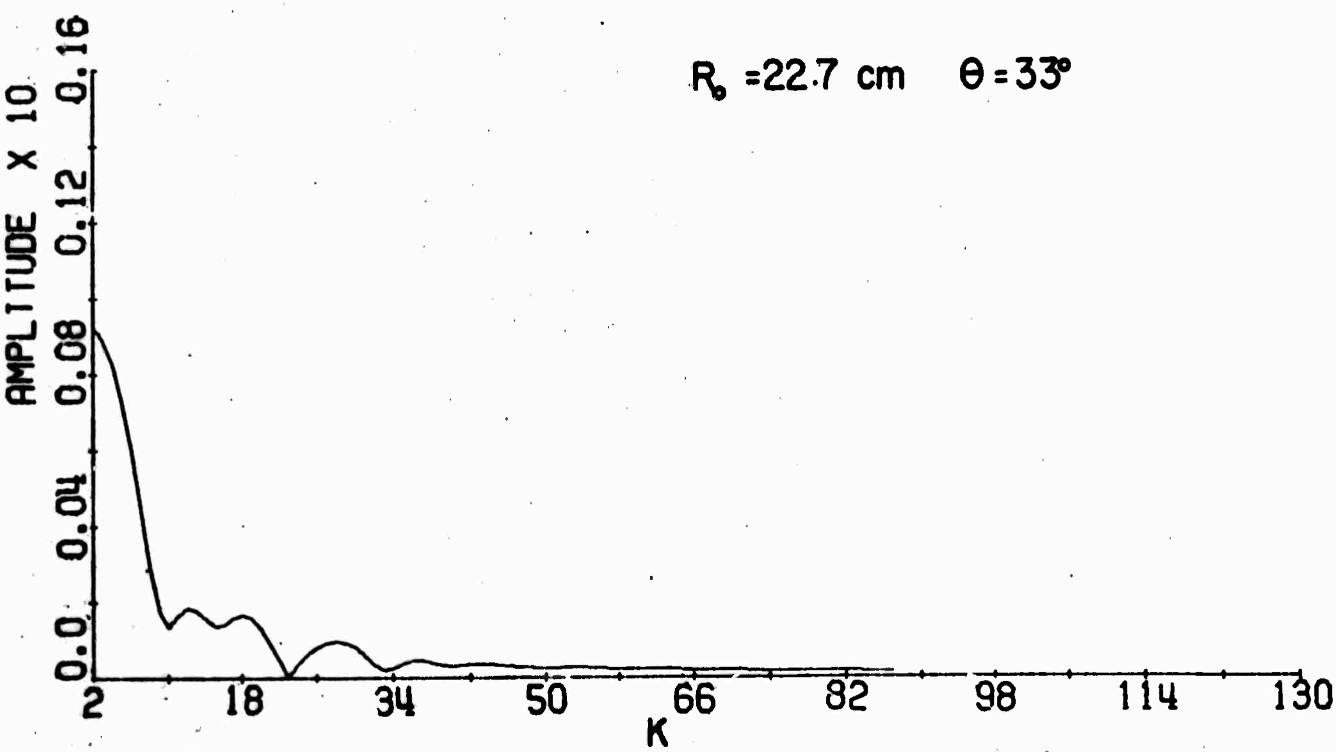

AMPLITUDE X 10
0.0 0.04 0.08 0.12 0.16
R₀ =22.7 cm θ = 33°
2 18 34 50 66 82 98 114 130
K

FIG. 9

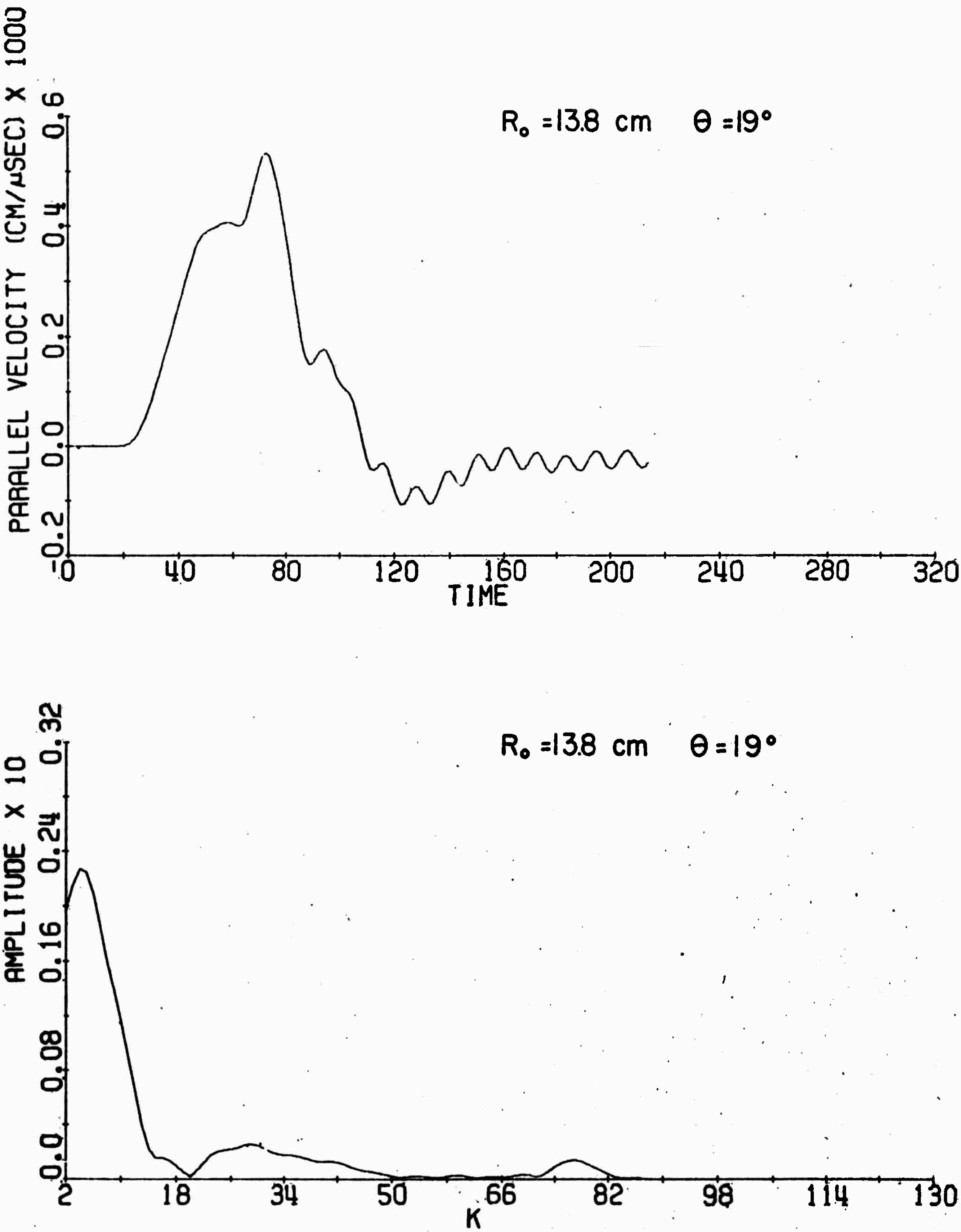

R_o =13.8 cm θ =19°
PARALLEL VELOCITY (CM/μSEC) X 1000
-0.2
0.0
0.2
0.4
0.6
0
40
80
120
160
200
240
280
320
TIME
R_o =13.8 cm θ =19°
AMPLITUDE X 10
0.0
0.08
0.16
0.24
0.32
2
18
34
50
66
82
98
114
130
K

FIG 10

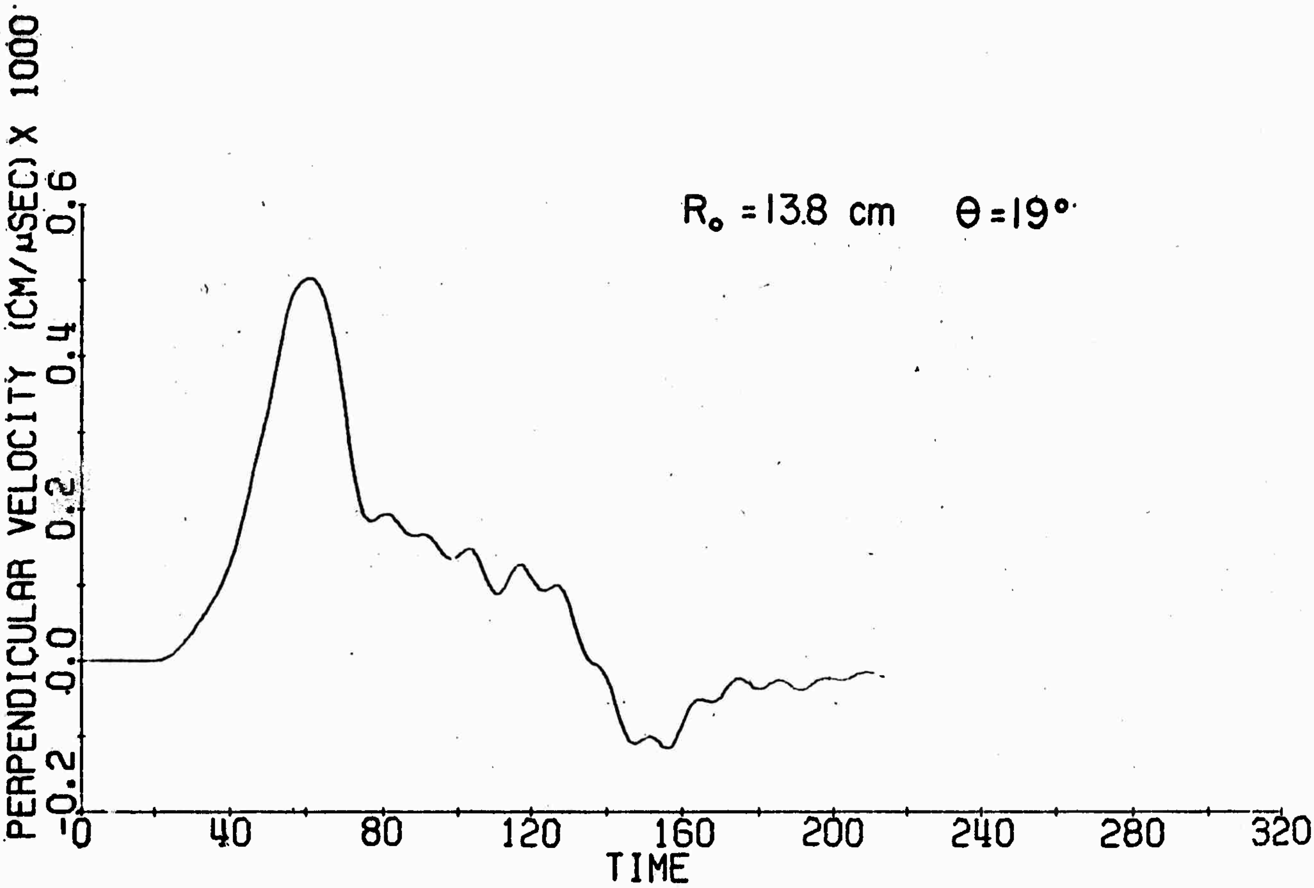

PERPENDICULAR VELOCITY (CM/μSEC) X 1000
-0.2
0.0
0.2
0.4
0.6
R_o =13.8 cm θ=19°
0
40
80
120
160
200
240
280
320
TIME

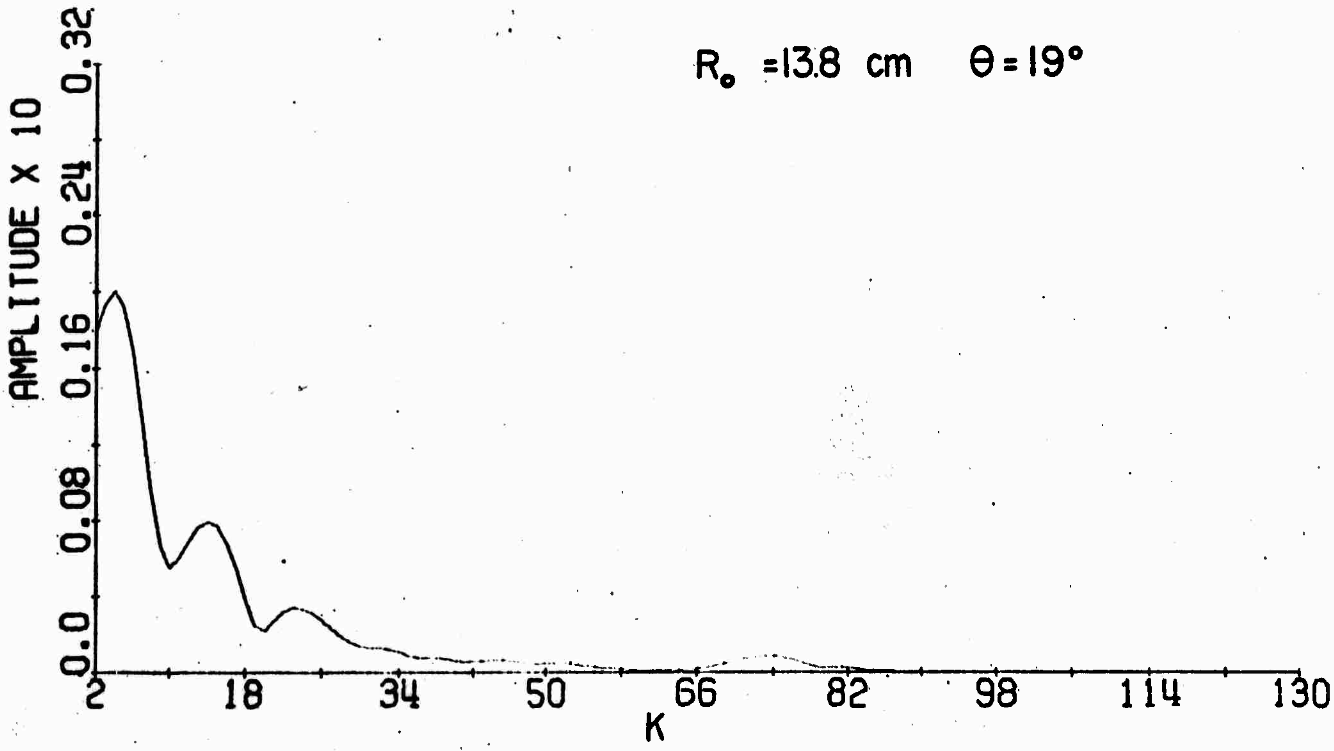

AMPLITUDE X 10
0.0
0.08
0.16
0.24
0.32
R_o =13.8 cm θ=19°
2
18
34
50
66
82
98
114
130
K

FIG 11

DOCUMENT CONTROL DATA - R & D

(Security classification of title, body of abstract and indexing annotation must be entered when the overall report is classified)

1. ORIGINATING ACTIVITY (Corporate author)

New Mexico Institute of Mining and Technology
Campus Station
Socorro, New Mexico 87801

2a. REPORT SECURITY CLASSIFICATION

UNCLASSIFIED

2b. GROUP

3. REPORT TITLE

A FOURIER ANALYSIS OF THE NEAR FIELD VELOCITIES RESULTING FROM A SIMULATED BILATERAL SHEAR FRACTURE

4. DESCRIPTIVE NOTES (Type of report and inclusive dates)

Scientific Final

5. AUTHOR(S) (First name, middle initial, last name)

Merle E. Hanson
Allan R. Sanford
Ronald J. Shaffer

6. REPORT DATE

January 1971

7a. TOTAL NO. OF PAGES

24

7b. NO. OF REFS

3

8a. CONTRACT OR GRANT NO.

F44620-70-C-0055

b. PROJECT NO.

AO 1031-4

c.

62701D

d.

9a. ORIGINATOR'S REPORT NUMBER(S)

9b. OTHER REPORT NO(S) (Any other numbers that may be assigned this report)

10. DISTRIBUTION STATEMENT

1. This document has been approved for public release and sale: its distribution is unlimited.

11. SUPPLEMENTARY NOTES

TECH, OTHER

12. SPONSORING MILITARY ACTIVITY

Air Force Office of Scientific Research
1400 Wilson Boulevard (NPG)
Arlington, Virginia 22209

13. ABSTRACT

The data from a numerically simulated dynamic bilateral shear fracture was analyzed using Fourier spectral techniques. The holes in the amplitude spectrums of the velocity data in the near field are compared with an analytically calculated source time. The periods resulting from the holes in the amplitude spectrum correlate with the source time calculated from analytical considerations. The analysis of the near field velocities at an observation point can show at least part of the characteristics of the finite source.

14. KEY WORDS	LINK A		LINK B		LINK C	
	ROLE	WT	ROLE	WT	ROLE	WT
Dynamic Shear Fracture Fourier Spectrum Amplitude Sepctrum Source Time						